Is the Stratospheric QBO affected by Solar Wind Dynamic Pressure via an Annual Cycle Modulation?

Hua Lu[a,1], and Martin J. Jarvis[a]

Prepared for Journal of Geophysics Research

Revised December 2010

[1]Corresponding author Email: hlu@bas.ac.uk
[a] Hua Lu, Martin. J. Jarvis, British Antarctic Survey, High Cross, Madingley Road, Cambridge CB3 0ET, United Kingdom. (email: hlu@bas.ac.uk; mjja@bas.ac.uk)

Abstract: In this study, statistical evidence of a possible modulation of the equatorial stratospheric Quasi-biennial Oscillation (QBO) by the solar wind dynamic pressure is provided. When solar wind dynamic pressure is high, the QBO at 30-70 hPa is found to be preferably more easterly during July to October. These lower stratospheric easterly anomalies are primarily linked to the high frequency component of solar wind dynamic pressure with periods shorter than 3-years. In annually and seasonally aggregated daily averages, the signature of solar wind dynamic pressure in the equatorial zonal wind is characterized by a vertical three-cell anomaly pattern with westerly anomalies both in the troposphere and the upper stratosphere and easterly anomalies in the lower stratosphere. This anomalous behavior in tropical winds is accompanied by a downward propagation of positive temperature anomalies from the upper stratosphere to the lower stratosphere over a period of a year. These results suggest that the solar wind dynamic pressure exerts a seasonal change of the tropical upwelling which results in a systemic modulation of the annual cycle in the lower stratospheric temperature, which in turn affects the QBO during Austral late winter and spring.

1. Introduction

The quasi-biennial oscillation (QBO) of the equatorial stratosphere is characterized by alternating easterly and westerly wind regimes and dominates the variability of the tropical lower stratosphere [*Naujokat*, 1986; *Baldwin et al*., 2001]. The winds descend from 10 hPa to 100 hPa at an averaging speed of 1 km/month and repeat at intervals from 18-36 months, with an average periodicity of ~28 months [*Pascoe et al*., 2005]. Our current understanding of the QBO is largely based on the theoretical augment of *Holton and Lindzen* [1972] who showed how vertically propagating equatorial waves are absorbed at a critical layer by the mean flow and in turn generate alternating acceleration of the zonal flow in either easterly or westerly directions [*Plumb and Bell*, 1982].

In addition to this wave-driven mechanism, seasonal or interannual variation of the QBO may also arise from seasonal changes in tropical upwelling [*Dunkerton*, 1991; 2000; *Holton et al*., 1995; *Kinnersley and Pawson*, 1996], shifting of latitudinal gradients in the subtropics [*Randel et al*., 1998], or variation of the semi-annual oscillation (SAO) in the tropical upper stratosphere [*Dunkerton and Delisi*, 1997]. Additional temperature change may be caused by the secondary circulation, induced by the QBO itself, which consists of an increase in the upwelling at the easterly shear zone and a suppression of the upwelling at the westerly shear zone [*Plumb and Bell*, 1982].

While the QBO is primarily driven by internal wave dynamics, a possible modulation of the QBO *via* external forcing cannot be ruled out. There is increasing evidence that part of variability in the stratosphere may be linked to the solar activity [*Haigh*, 2003; *Labiztke et al*., 2006; *Lockwood et al*., 2010; *Gray et al*., 2010]. Studies have indicated that solar variability may indirectly modulate the QBO through the variation in solar UV irradiance [*Salby and*

Callaghan, 2000; *Soukharev and Hood*, 2001; *McCormack*, 2003; *Mayr et al*., 2005; 2006; *McCormack et al*., 2007]. Absorption of solar ultraviolet (UV) radiation by ozone may cause changes in temperature and hence in the QBO near the equatorial stratosphere [*Hood*, 2004; *Crooks and Gray*, 2005; *Pascoe et al*., 2005]. Such anomalous heating in the upper stratosphere may alter Rossby wave propagation and breaking [*Cordero and Nathan*, 2005; *McCormack et al*., 2007] and hence cause an indirect dynamic feedback through modulation of the polar vortex and the Brewer-Dobson (BD) circulation [*Kodera and Kuroda*, 2002]. *Salby and Callaghan* [2000] examined the radiosonde equatorial zonal wind at 45 hPa for the period of 1956–1996 and found that the average duration of the westerly QBO (wQBO) around solar maxima is ~3–6 months shorter than that around solar minimum. *Soukharev and Hood* [2001] performed composite analysis using the radiosonde-derived equatorial zonal wind at 50 to 10 hPa from 1957 to 1999 and found that the duration of both QBO phases was shorter at solar maxima than at solar minima. Using ECMWF ERA-40 reanalysis, *Pascoe et al.* [2005] found that the average time required for the eQBO to descend from 15 hPa to 44 hPa is ~2 months less at solar maxima than at solar minima. By using a fully interactive 2D Chemical/Dynamical Model, *McCormack* [2003] and *McCormack et al.* [2007] found that the duration of the wQBO can be 1-3 months shorter at solar maximum than solar minimum. They suggested that the ozone heating induced by solar UV in the upper stratosphere reduces the tendency for a westerly wind and hence produces an anomalously stronger easterly wind in the tropical upper stratosphere. By generating the QBO internally using a high resolution general circulation model (GCM), *Palmer and Gray* [2005] showed that the durations of both QBO phases may be reduced by up to 2 months at solar maximum. *Cordero and Nathan* [2005] showed that prescribing higher solar UV inputs produces a QBO with shorter duration and larger amplitude. In addition to the direct ozone heating, wave-ozone feedback has been shown to modify the refraction of tropical quasi-stationary Rossby waves, reducing the tropical upwelling and resulting in faster descent of eQBO [*Nathan and Cordero*, 2007]. *Mayr et al.* [2006] prescribed a synthetic period of 10-years with varying amplitude of radiative forcing at three different heights (0.2% – surface, 2% – 50 km, 20% –100 km) and their model simulation also resulted in a modulation of the QBO in the stratospheric equatorial region which appeared to be generated by this synthetic SC modulation. *Mayr et al.* [2005] suggested that an annual oscillation can originate near 60 km, through which the prescribed 10-year modulation could be transferred downward and amplified by tapping the momentum from the upward propagating gravity waves.

In contrast, other studies have been unable to find a significant link between solar UV and QBO variability. *Hamilton* [2002] used data from 1950 to 2000 and found a quasi-decadal variation in the duration length of the wQBO at 40-50 hPa but the connection with the 11-year solar cycle noted by *Salby and Callaghan* [2000] did not always hold and the correlation coefficient was only –0.1 when computed over a longer period which included 22 westerly phases. *Fischer and Tung* [2008] used radiosonde measurements for 1953-2005 and showed that the correlations between the duration of the QBO and the 11-yr SC for either phase of the QBO were close to zero. In addition, oppositely-signed correlations were found to exist in the pre-1990 and post-1990 periods. More recently, *Kuai et al.* [2009] also dismiss the solar cycle modulation of the QBO period. With exceedingly long model runs, those authors found that a strong synchronization of the QBO period with integer multiples of the Semi-Annual Oscillation (SAO) in the upper stratosphere may generate ‘‘decadal’’ variability in the QBO period causing a waxing and waning of the correlation between solar forcing and the QBO period. They therefore suggested that the SC-QBO duration relationship reported previously reflects only a chance behaviour resulting from the use of relatively short observational records.

In addition to solar UV, signature of the solar wind streaming out from the Sun has also been found in various climate records [*Lu et al*., 2008a; *Lockwood et al*., 2010a,b; *Woollings et al*., 2010]. The solar wind variability manifests itself at Earth in a number of ways but most prominently through geomagnetic activity, thermospheric heating and the aurorae. Observational studies have shown that the solar wind induced geomagnetic activity may alter stratospheric chemistry indirectly through particle precipitation [*Solomon et al*. 1982; *Randall et al*., 2005; 2007; *Seppälä et al*. 2007; *Siskind et al*., 2007]. Chemical-dynamical coupled general circulation models (GCMs) have indicated that odd nitrogen (NO_x) induced by energetic charged particle precipitation during geomagnetic storms may cause temperature changes in both the polar and equatorial regions and in the stratosphere and the troposphere [*Langematz et al*., 2005; *Rozanov et al.*, 2005; *Seppälä et al*. 2009].

Other studies suggested that solar wind induced geomagnetic activity may perturb atmospheric circulation through a change in planetary wave reflection conditions [*Arnold and Robinson*, 2001; *Lu et al*. 2008b]. Model simulations by *Arnold and Robinson* [2001] have indicated that a change in planetary wave reflection conditions at the lower thermospheric boundary caused by thermsopheric heating induced by solar wind driven geomagnetic activity can reduce planetary wave propagation into the stratosphere, leading to a strengthening of the stratospheric polar vortex and a weakening of the BD-circulation. Significant correlations have also been established between geomagnetic activity and lower stratospheric temperature by *Lu et al*. [2007]. They found that the temperature response to the 11-yr SC and geomagnetic Ap index tend to enhance each other in the tropical upper troposphere and lower stratosphere, the magnitude of the response to geomagnetic activity being slightly larger than that associated with the 11-yr SC. *de Artigasa and Elias* [2005] have shown that, when solar flux is high, the eQBO (at 15-50 hPa) is more likely to be associated with high geomagnetic activity and the wQBO is more likely to be associated with low geomagnetic activity; at solar minimum, this relationship is reversed. *Lu et al*. [2008a] have shown that there is a robust relationship between solar wind dynamic pressure and the zonal wind and temperature in the northern polar winter. Stratospheric wind and temperature variations are positively projected onto the Northern Annular Mode (NAM) when the 11-yr SC is at its maximum phase, and negatively projected onto the NAM during the 11-yr SC minimum phase. This implies a weakening of the BD-circulation with reduced upwelling into the lower stratosphere at low-latitude under high solar wind forcing, consistent with the tropical warming signals detected by *Lu et al.* [2007].

While variations in solar radiation are most strongly seen in the 11-year solar cycle, the solar wind induced geomagnetic activity exhibits a strong variability at shorter time scales. *Lu et al*. [2008a] shows that the solar wind dynamic pressure and F10.7 solar flux are poorly correlated, largely due to those shorter time variations. Their weak statistical dependence allows the signals associated with the 11-year solar irradiance and the solar wind dynamic pressure to be separated. However, their mechanisms may not be mutually exclusive and they could be acting together to either enhance or cancel the overall atmospheric responses.

Motivated by these results and rather strong extra-tropical signals in NH winter and spring observed by *Lu et al*. [2008a], a statistical analysis is conducted here to study possible solar wind dynamic pressure perturbations near the tropics, with a primary focus on detecting possible solar wind perturbation of the QBO. We use solar wind dynamic pressure, instead of geomagnetic indices, because geomagnetic indices are measured through the interaction of the terrestrial environment with the solar wind and are therefore not completely independent of internal Earth atmospheric processes. For instance, *Sugiura and Poros* [1977] identified a QBO-like periodicity in the disturbed storm time current (Dst) and hence in geomagnetic activity, and *Jarvis* [1996] has shown a QBO periodicity in geomagnetic daily range induced by the semidiurnal tide. Conversely, the solar wind dynamic pressure is measured well outside of Earth's magnetosphere and is therefore wholly independent to the internal variability of the Earth's atmosphere. Nevertheless, it can be shown that similar but slightly weaker results are obtainable by using geomagnetic *Ap* index.

2. Data and Methods

In this study, daily QBO is defined as the deseasonalized daily zonal-mean zonal wind averaged over the latitude band of 5°S-5°N for five pressure levels at 70, 50, 30 20 and 10 hPa. Zonal-mean zonal winds are extracted from the ECMWF (European Centre for Medium Range Weather Forecasting) ERA40 Reanalysis (September 1957 to August 2002) and ECMWF Operational analyses (September 2002 to December 2009). The ERA-40 Reanalysis was assimilated using direct radiosonde and satellite measurements [*Uppala et al*., 2005]. It has a spectral resolution of T159, corresponding to a 1.125º horizontal resolution in latitude and longitude and are available at 23 standard pressure surfaces from 1000 hPa to 1 hPa. The ECMWF Operational data were output from the ongoing analyses produced by the most recent ECMWF Integrated Forecasting System (IFS) model. Data from September 2002 to the present day are available on the same 1.125º grid and but on 21 pressure levels (before 07/11/2007) and 25 pressure levels (since 07/11/2007). The ERA-40 and the Operational data sets share 21 pressure levels; the exceptions are four levels in the lower troposphere (*i.e*. 600, 775, 900, and 950 hPa) which are excluded from this analysis. Nevertheless, the two data sets share the same five pressure heights where the QBOs are estimated.

It has been established that before the satellite era (*i.e*. before September 1978), the scarcity of SH radiosonde measurements and lack of direct measurement at altitudes above 10 hPa resulted in unreliable estimations in ERA-40, particularly in the southern hemisphere and in the upper stratosphere. In the tropics, however, *Baldwin and Gray* [2005] showed that the QBO extracted from ERA-40 is consistent with rocketsonde winds (that were not assimilated by ERA-40) measured at Ascension and Kwajalein up to the 2-3 hPa altitude level, even for those years before the satellite era. *Pascoe et al.* [2005] also found that the ERA-40 accurately describes the QBO and the tropical stratospheric circulation. We also compared the monthly averaged QBO with those available at the Free University of Berlin (FUB) [*Naujokat*, 1986] for the five pressure levels used here. The two data sets are in good agreement with a correlation coefficient greater than 0.9 for all five pressure levels. In addition, the response to solar wind dynamic pressure reported in this paper is found primarily below 10 hPa. Hence, for these reasons, the results reported here make use of all available data since 1963. Figure 1 shows latitudinally integrated zonal-mean zonal wind at 5°S-5°N as a function of height (1-100 hPa) for the period of 1958-2009.

[insert figure 1 here]

The upper two panels of figure 1 display the original monthly mean data while the lower two panels show its deseasonalized anomalies. A prominent Semi-Annual Oscillation (SAO) exists near the stratopause level when the data is not deseasonalized. Once deseasonalization is applied, the descending alternating easterly and westerly winds of the QBO are the dominant feature, with maximum amplitude of ~40 m s^{-1} at ~3-5 hPa, where the QBO is initialized. In the upper stratosphere, discernible enhancement of easterly anomalies occurred in the 1970s while an enhancement of westerly anomalies occurred from the mid- 1980s to the late 1990s. From 2000 onwards, it becomes comparable to the earlier pattern again. It has been suggested that the enhanced westerly anomalies seen in the upper stratosphere during the 1980s and 1990s might be a result of data assimilation pre-/post- satellite era [*Punge and Giorgetta*, 2007]. The extended data seem to suggest it is more likely to be a real phenomenon in which a multi-decadal variation is superimposed upon the upper stratospheric SAO.

Solar wind dynamic pressure (P_{sw}) measured in Geocentric Earth Magnetic (GEM) coordinates is obtained from the NASA-OMNI site (http://omniweb.gsfc.nasa.gov/). This data set is produced from solar wind and interplanetary magnetic field measurements from 15 geocentric satellites and 3 spacecraft in orbit around the L1 Sun-Earth Lagrange point and has been carefully compiled through cross-calibration. P_{sw} has been calculated by NASA-OMNI as $P_{sw} = 1.6726 \times 10^{-6} N_{sw} V_{sw}^2$, where N_{sw} is the flow density in number of particles per cm^3 and V_{sw} is the solar wind speed in km s^{-1}. In physical terms, P_{sw} represents the momentum flux of the solar wind and has a unit of nPa (nano Pascals). Daily averages of solar wind P_{sw} from January 1963 to December 2009, covering ~4.5 solar cycles, together with its monthly mean are used here. The main advantage of using the daily data over the monthly mean is that the downward decent of the signals can be studied in more detail.

There are a few missing data periods of P_{sw} due to inappropriate positioning of satellites or instrument failure. For instance, before August 1965, and also between September 1982 and October 1994, the data availability is below 50% at hourly resolution, with 8–15 complete days showing as missing data in each month [*King and Papitashvili*, 2005]. For up to 3 days of missing values, a simple interpolation is used to fill the gap. For longer missing data periods, no treatment is applied and those days are ignored by the analysis. For the months with more than 15 day missing values, monthly P_{sw} is treated as missing data. The effect of missing data for running composite/regression is that different months or seasons under investigation may involve different sample lengths. While the monthly P_{sw} varies from 1.2 to 6.7, the daily P_{sw} varies from 0.1 to 27 nPa with an arithmetic mean value of 2.5 nPa and standard deviation of 1.5 nPa (not shown).

Figure 2 shows monthly mean P_{sw} and its high and low frequency components, where the separation cutoff period is 36-month. The low frequency P_{sw} shows a quasi-decadal variation superimposed on a slow varying trend. Its quasi-decadal variation peaks at the minimum phase of the 11-year solar cycle suggesting an 11-year solar cycle modulation on P_{sw}. There is clear evidence of slow-varying 11-year cycle in its high frequency component. Nevertheless, over the period 1963-2009, the correlation coefficient between P_{sw} and sunspot number or F10.7 solar flux is below 0.1 on a daily timescale and remains below 0.2 for the monthly mean. This is largely due to the high frequency variation of P_{sw}. Thus, any significant P_{sw}, signals especially those associated with its high frequency component, should be fairly statistically independent to the signature associated with the 11-year solar cycle.

[Insert figure 2 here]

For simplicity, we use $\bar{P}_{sw} < -0.25$ and $\bar{P}_{sw} > 0.25$ to define low and high solar wind dynamic pressure either for the raw P_{sw} or its high frequency component, where $\bar{P}_{sw}$ stands for the median-normalized values of P_{sw}; transition periods where $|\bar{P}_{sw}| \leq 0.25$ are excluded. The same rule is applied to differentiate the westerly and easterly QBO phases. Qualitatively similar results can be obtained if other definitions, such as mean instead of median for $\bar{P}_{sw}$, are used. Hereinafter, high and low solar wind dynamic pressure are abbreviated as HP and LP.

3. Results

3.1 Perturbations caused by Solar Wind Dynamic Pressure

Figure 3 shows the QBO phase occurrence by month as a percentage separated into high (upper panel) and low (lower panel) solar wind dynamic pressure for 70hPa (left), 50 hPa (central) and 30hPa (right) estimated using daily data. Under HP, the difference in occurrence between eQBO and wQBO is noticeably smaller than it is under LP at all three pressure levels and the difference even reverses at 30 hPa. The largest difference occurs under LP conditions during the Austral winter and spring and reduces with increasing altitude. The departure between the QBO phase occurrence under HP and LP begins in June to July. By assuming that both the QBO and P_{sw} follow a first-order auto-regressive (AR1) process, we use a Monte Carlo trial-based test [*Wang et al.*, 2006] to determine the significance of the differences. It is found that the differences under LP at 50 hPa and 70 hPa are significant at the 95% confidence level only for July to October while the difference at 30 hPa are significant at the 95% for almost the entire year (except December and January). As a whole, the behavior of the QBO phase occurrence differs from January to June, when the occurrence of wQBO hardly changes from LP to HP, to July to December when the occurrence of wQBO increases and the occurrence of eQBO decreases significantly under LP. This suggests a higher eQBO to wQBO occurrence ratio in the lower stratosphere under HP than under LP conditions. It suggests that under HP conditions there is either anomalously more eQBO descent down from higher altitudes or a slower descent rate of the eQBO at 30-70 hPa. The difference becomes weaker and not significant at higher altitudes.

[Insert Figure 3 here]

The same conclusion can be reached if the QBO phase occurrence is grouped according to QBO phase and then the occurrence percentages calculated for HP and LP conditions (see figure 4). At 70 hPa during September, nearly 50% of eQBO occurrence takes place under HP compared with only 20% under LP; the difference becomes considerably smaller for wQBO. The differences under eQBO for August-October for the all three pressure levels from 30 to 70 hPa are significant at the 95% confidence level or above and at the 90% confidence level for July. This confirms that significantly more eQBO occurred in the lower stratosphere during the Austral late winter and spring and a positive relationship exists between P_{sw} and increased eQBO occurrence.

[Insert Figure 4 here]

Figure 5a shows the vertical profile of annual mean equatorial zonal wind (solid line) plus and minus its one standard deviation. Greater variability exists in the stratosphere than in the troposphere largely due to the QBO. Figure 5b;c;d shows the vertical profile of tropical zonal wind anomalies for separated HP and LP conditions under three different sampling conditions, *i.e.* for (b) for 1963-2009, (c) for 1979-2009 and (d) for 1963-2009 but with volcanic eruption affected data excluded. All the vertical profiles of zonal wind anomalies are calculated by using daily deviation from its long-term mean and then aggregating to its annual average. It shows that the modulation of solar wind dynamic pressure on daily equatorial zonal wind is marked by a vertically 3-cell structure with westerly anomalies (~0.3-0.5 m s^{-1}) in the troposphere, easterly anomalies (~2 m s^{-1}) at 20-70 hPa and westerly anomalies (~3 m s^{-1}) at 3-10 hPa under HP-LP. As a whole, this vertical structure accounts for ~5-10% of one standard deviation of the tropical zonal wind for each associated vertical region and these wind differences are significant at the 95% confidence level. Changing the data period from 1963-2009 (figure 5b) to 1979-2009 (figure 5c) or excluding the years affected by major volcanic eruptions (figure 5d) does not alter its general pattern or significant levels. Similar results can also be obtained by excluding the years affected by the major Niño events.

[Insert Figure 5 here]

Figure 6 shows that the same vertical profile of equatorial zonal wind anomalies also holds on a seasonal time scale and the general vertical structure remains across all four seasons (*i.e.* December-February, March-May, June-August, and September-November). In the lower stratosphere, the largest and most significant departure from zero wind occurs during Austral winter (June-August). A closer examination also suggests that there is a noticeable seasonal variation in its vertical structure. From December to February, an upward shift is obtained for the bottom cell of the stratosphere; from September to November, a downward shift is apparent for both top and bottom cells in the stratosphere. The largest differences between HP and LP conditions in the upper stratosphere occur in SON and DJF while in the lower stratosphere they occur in MAM and JJA. Similar results can also be obtained by excluding the years affected by either the major Niño events or the major Volcanic eruptions.

[Insert Figure 6 here]

Figure 7a shows the 31-day running composite difference (HP – LP) of the equatorial zonal mean zonal wind from June to October. Significant easterly anomalies (~8 m s^{-1}) are found in 30-70 hPa pressure levels while westerly anomalies (~1 m s^{-1}) are simultaneously detected in the upper troposphere. It is apparent that the stratospheric easterly anomalies descend from 10 hPa or above from June and become significant from late July to early October. Figure 7b shows the same running composite difference except that a high pass filter with a cut-off period of 1095-days (~3 years) is applied to the daily P_{sw}. Note that both the strength of the composite difference and the statistical confidence level are enhanced in the stratosphere, suggesting that not the decadal-scale variability of P_{sw} but the variation of P_{sw} at periods below 3 years is responsible for the easterly anomalies at 30-50 hPa. Longer term variation of P_{sw} appears to be responsible to the anomalies at and below 70 hPa.

[Insert Figure 7 here]

The radiative heating induced by volcanic aerosols may also influence the lower stratospheric temperature which in turn may lead to stalling of the downward propagation of the QBO [*Dunkerton*, 1983]. To examine possible contamination by the temporary heating caused by volcanic aerosols, Figure 7c shows the same composite difference as Figure 7b but with the major volcanic affected data (*i.e.* Agung in March, 1963, El Chichón in March, 1982, and Pinatubo in June, 1991) excluded. A quantitatively similar result is obtained, suggesting that those easterly anomalies in the lower stratosphere are not strongly biased by the major volcanic induced warming in the lower stratosphere. Note that there are quite a lot of missing data in the daily P_{sw} during 1963, 1964, 1982 and 1983 (see figure 2), the contamination of those years are already excluded in the analysis of figure 7a;b, meaning that the data affected by Pinatubo volcanic eruptions are the only difference between figure 7b and 7c.

It has been observed that ozone concentrations and temperature in the tropical lower stratosphere (~70 hPa) are anomalously low during the El Niño phase of the El Nino – Southern Oscillation (ENSO) [*Randel et al.*, 2009]. To examine possible bias due to the large cooling effect caused by the major El Niño events, figure 7d shows the same analysis as figure 7b but with the major El Niño (*i.e.* 1972, 1973, 1982, 1983, 1997, and 1998) affected years excluded. Note that, due to missing P_{sw} in 1982 and 1983, the data affected by 1972, 1973, 1997 and 1998 represent the only difference between figure 7b and 7d. Again a quantitatively similar result is obtained, suggesting that the major El Niño events do not alter the QBO- P_{sw} relationship significantly.

Figure 8 summarizes the effect of the higher frequency (< 3-yrs, the red line in figure 2) components of P_{sw} on the QBO at 50 hPa and 30 hPa (figure 8a;d), where both P_{sw} and the QBO are averaged from July to October. These pressure levels and months are chosen because the results shown in figures 3, 4 and 7 suggest the largest effect of P_{sw} on the QBO at those levels and during those months. At both pressure levels, there are significant negative correlations between mean P_{sw} and the mean QBO. Neither Volcanic eruption nor El Niño affected years are found to dominate or alter the correlations significantly. This helps to rule out a possible linear contamination of the QBO- P_{sw} relationship by volcanic eruption and the major El Niño events. However, it does not rule out the possibility that the ENSO might modulate the QBO- P_{sw} relationship through non-linear processes and a possibility modulation in other calendar months or at different frequency. This is beyond the scope of the current study.

[Insert Figure 8 here]

Figure 9 shows the running composite HP − LP difference of the equatorial zonal mean temperature from January to December. The largest positive anomalies (~2 K) are found from August to November at 30-50 hPa. Positive anomalies (~ 1 K) are also found at 70-150 hPa (becoming significant between 100 and 150 hPa) during the December to June period while significant negative anomalies (~ 0.5 K) are detected at 300-700 hPa between July and October. The two most striking and significant features of figure 9 are: 1) downward propagation of positive temperature anomalies in the upper stratosphere from December of the previous year to the lower stratosphere in December of the following year; 2) the anomalous warming at ~100 hPa during the Boreal winter and spring and anomalous cooling at 700-300 hPa during the Austral winter. The combined effect of these temperature anomalies is a systematic annual modulation of the annual oscillation of temperature in the lower stratosphere related to solar wind dynamic pressure.

[Insert Figure 9 here]

Such annual cycle modulation can be compared to the annual oscillation normally present in the stratosphere. Figure 10a shows the climatological mean annual pattern of the tropical zonal mean zonal wind. The strongest variation appears in the upper stratosphere (1-5 hPa) with a semi-annual cycle clearly visible. In the lower stratosphere (50-100 hPa), a weaker semi-annual cycle also exists and this is roughly in phase of that in the upper stratosphere. In addition, there is a pronounced annual cycle both in the upper and lower stratospheres. In the upper stratosphere, the annual cycle is marked by nearly 3 times stronger easterly winds in the Boreal winter (~40 m s^{-1}) than in the Austral winter (~15 m s^{-1}). In the lower stratosphere, the situation reverses with weaker easterlies occurring in the Boreal winter (~2 m s^{-1}) and stronger easterlies in the Austral winter (~5 m s^{-1}). In the 10-50 hPa region where the QBO prevails, the magnitude of zonal mean wind is primarily easterly (~15 m s^{-1}). It also shows a modulation by an annual cycle, albeit weak, with stronger easterly winds occurring in the Austral winter.

[Insert Figure 10 here]

Figure 10b shows the temperature anomaly (shaded contours) compared to the climatological altitude dependent mean value of tropical zonal mean temperature (thick solid lines). In the upper stratosphere, similar to the winds, the SAO dominates. The amplitude of temperature there during the Boreal winter and spring (4-5 K) is about twice as large as it is in Austral winter and spring (2-3 K), implying an additional annual cycle influence. An annual cycle dominates at 50-100 hPa with a magnitude of –3 K during the Boreal winter and 4 K in Austral winter, a peak-to-peak value of ~8 K at 70 hPa. The semi-annual cycle in the upper and the annual cycle in the lower stratosphere oppose each other during the Austral winter, resulting in a close to flat temperature climatology at ~20 hPa. The climatological tropical mean wind and temperature compare well with previously studies [*Baldwin et al.*, 2001; *Pascoe et al.*, 2005; *Fueglistaler et al.*, 2009].

Thus the annual oscillation linked to solar wind dynamic pressure (figure 9) works in opposition to the normal annual oscillation in the lower stratosphere (*i.e.* 50-100 hPa), reducing its amplitude. It is possible that, because the eQBO is most sensitive to diabatic change in the lower stratosphere and particularly to temperature changes near the tropopause [*Kinnersley and Pawson*, 1996], the modulation effect of solar wind dynamic pressure is stronger for eQBO than for wQBO.

The seasonal variations of the equatorial wind and temperature anomalies in relation to the variation of solar wind dynamic pressure can also be compared with the seasonal statistics of QBO phase transitions. Figure 11 shows every major phase transition of the QBO between

1953 and 2009 at five different pressure levels grouped by months into histograms, where the transitions before 1958 were determined by using deseasonalized monthly radiosonde data and after 1958 were based daily data. The months where the transitions occurred may differ by a month or two when compared to the earlier findings [*Dunkerton*, 1990; *Baldwin et al.*, 2001; *Hampson and Haynes*, 2004; *Christiansen*, 2010] as our deseasonalization is based on extended daily (instead of monthly) data from 1958-2009. In terms of the general distribution of the transitions, they remain similar to the previous studies based on radiosonde estimates, especially at 50 hPa. At 30 hPa, the peak of the phase transition tends to occur about two months earlier than those based on monthly NCEP reanalysis [see fig. 1 of *Hampson and Haynes*, 2004].

The histograms of transitions at 30-70 hPa show a noticeable annual cycle variation for both QBO phases. It is clear from Figure 11 that at 30 and 50hPa the transitions occur less often from July to November than other months. The months and pressure levels with reduced QBO phase transition coincide with the period/the height when/where the effect of solar wind dynamic pressure on both equatorial zonal wind and temperature is most significant (see figures 9 and 7). Similarly, the transitions of both the QBO phases at 10 hPa occurred far less often during NH winter and spring than during other months. Again, this coincides with the period when solar wind dynamic pressure related positive temperature anomalies were found to be present at that pressure level and above (see figure 9).

[Insert Figure 11 here]

4. Discussions

The variability of the stratospheric QBO is known to be largely characterized by the "stalling" of easterly QBO (eQBO) near 30 to 50 hPa as the easterly shear zone tends to descend more irregularly than the westerly shear zone [*Naujokat*, 1986]. Modeling simulations have suggested that the “stalling” of the QBO depends critically on whether deposition of easterly momentum at the equator is sufficient to overcome the tendency for the easterly shear zone to be advected upward or held static by the combination of the BD-circulation and the QBO-induced residual circulation [*Dunkerton*, 1991; 2000; *Kinnersley and Pawson*, 1996]. The tropical upwelling of the BD-circulation acts to slow down the descent rate of the QBO and consequently extends the QBO period, or increases the occurrence frequency for a given QBO phase. Because of the QBO-induced residual circulation, the effect of the tropical upwelling on the descent of the shear zone depends on the QBO phase. Upward motion is associated with eQBO [*Plumb and Bell*, 1982]: it strengthens the upwelling so that the descent of the easterly shear zone is slowed further. Conversely, downward motion is associated with wQBO: it causes cancellation of the tropical upwelling so that the BD-circulation imposes a smaller slowing effect on the descent of westerly shear zone. As a whole, the descent rate of the wQBO is less affected by variations associated with the BD-circulation than that of the eQBO [*Kinnersley and Pawson*, 1996; *Dunkerton*, 2000; *Hampson and Haynes*, 2004].

The annual variation of the QBO may arise from a seasonal variation of the BD-circulation, which is explained by the ‘‘extratropical stratospheric pump’’ mechanism [*Holton et al*., 1995]. This is dynamically driven by momentum dissipation of extratropical waves so that air is drawn upward from the tropical troposphere and then poleward and downward at high latitudes causing a seasonal variation in the BD circulation [*Yulaeva et al*., 1994]. The periods with stronger overturning require stronger diabatic heating at the ascending branch and cooling at the descending branch, which cools the stratosphere in the tropics and warms it in the polar region. Because the planetary wave drag in the stratosphere is stronger in the northern hemisphere (NH) winter than in the southern hemisphere (SH) winter, it drives stronger upwelling and lower temperatures in the tropical lower stratosphere during NH winter. As a result, the descent of the eQBO is preferentially stronger during the months of May to July, when the tropical upwelling in the lower stratosphere is weakest [*Baldwin et al*., 2001]. Here we show that, on top of the modulation due to the extratropical wave-driven BD-circulation, solar wind dynamic pressure may also perturb the tropical zonal wind in the lower stratosphere and the largest effect is detected during July to October.

It is known that the annual cycle in lower stratospheric temperature plays an important role in the QBO phase transition and occurrence [*Fueglistaler et al*., 2009]. Previous studies have suggested that the annual synchronization of the QBO phase transition is linked to seasonally varying tropical upwelling [*Dunkerton*, 1990; *Hampson and Haynes* 2004] and the annual cycle is a consequence of faster (slower) tropical upwelling in the Boreal (Austral) winter [*Yulaeva et al*., 1994; *Holton et al*., 1995; *Rosenlof*, 1995]. More recent studies have however challenged the “extratropical pump mechanism” and have resulted in some debate regarding the processes driving upwelling in the tropical BD branch [*Fueglistaler et al*., 2009]. It has been shown by both observation and numerical calculation that tropical wave forcing produced by convective motion may also be partially responsible for the variation in the lower stratospheric temperature and the QBO [*Norton*, 2006; *Randel et al*., 2008; *Lu et al*., 2009; *Taguchi*, 2009]. Here, we present some statistical evidence of a possible modulation of the lower stratospheric annual cycle via solar wind dynamic pressure P_{sw} and the descent pattern of the QBO and tropical temperature anomalies. We show that there is a significant perturbation of tropical zonal wind, apparently related to P_{sw}, in both the stratosphere and the troposphere. Based on these results, we suggest that, in addition to atmospheric internal variability, solar wind driven modulation may also play a role in causing inter-annual variation in the strength and descent pattern of the QBO.

More recently, *Lu et al*. [2009] found that the processes that synchronize the QBO exert different effects on different QBO phases from season to season. During July and August, the phase speed is significantly slowed when westerlies prevail through the pressure levels, and becomes more irregular when easterlies are dominating there. They found that tropical upwelling alone is insufficient to explain the more irregular behaviour of the eQBO shear zone during SH winter and suggested that changes in tropical waves could be involved. A possible modulation of the QBO by solar wind dynamic pressure may provide a partial explanation for their observation. Our results on solar wind dynamic pressure related perturbation of the QBO add another element to this general picture of the QBO variability mechanisms. As tropical upwelling is generally lower during the Austral winter and spring, a seasonal temperature perturbation linked to high P_{sw} may create an environment which favours significantly more easterly shear zone to descend from higher altitudes into the lower stratosphere, and/or a slower descent of the QBO overall.

It is worth noting that the seasonal temperature change that we find to be related to solar wind dynamic pressure in the stratosphere is ~1 K in the lower stratosphere and ~2 K in the upper stratosphere. These values are comparable to the inter-annual variability of tropical temperature associated with ENSO, volcanic eruptions, and the QBO [*Randel et al*., 2004; *Fueglistaler et al*., 2009].

Our analysis of including or excluding the data affected by the major Volcanic eruptions or the major El Niño events showed no obvious bias on the statistically significant modulation of P_{sw} on the QBO. Nevertheless, more detailed study is needed to separate the effects of Volcano, ENSO, solar UV and solar wind. One obvious method is multivariate regression. However, the main drawback of such analysis is that these mechanisms may not be mutually exclusive and they could act together in a non-linear fashion to either enhance or cancel the overall responses. In addition, multivariate regression effectively reduces the degree of the freedom in the data and results in statistically less significant results. Thus, it remains technically challenging to separate the different origin/cause based on limited observational data, especially when the interaction is non-linear between the regressive variables.

Lu et al. [2008a] showed that the winter Northern Annular Mode (NAM) is positively correlated with P_{sw} when the 11-yr SC is at its maximum phase while negative correlation between P_{sw} and the stratospheric NAM exists in spring at solar minimum. Those extratropical signals suggested a weakening of the BD-circulation during winter months with reduced upwelling in the low-latitude lower stratosphere when both solar activity and solar wind dynamic pressure are high. The reversed relationship in spring implies enhanced BD-circulation and anomalous stronger upwelling at low latitudes. Our findings here (see figure 9) further confirm a seasonal modulation of the BD-circulation, reflected by a significant increase of tropical lower stratospheric temperature which corresponds to an anomalously weaker upwelling near the tropics. . It is also consistent with earlier findings of *Lu et al*. [2007] based on geomagnetic Ap index.

It should be noted that distinct differences exist in the extratropical and tropical responses. Firstly, the tropical response reported here does not change sign between winter and spring as opposed to the P_{sw} projection onto the NAM which tends to switch from positive to negative from NH winter to spring [*Lu et al*., 2008a]. Secondly, the tropical P_{sw} signals are independent of the 11-yr SC while conversely the extratopical signals are only statistically significant once the data are separated into high and low solar activity. Finally, a significant response of the QBO to the P_{sw} variation is detected during SH late winter and spring rather than during NH winter, when the most robust P_{sw} versus NAM relationship holds. Hence, there is no clear evidence to suggest that the tropical response is a direct result of the NH extra-tropical response reported previously by *Lu et al*. [2008a]. This implies that a change in extratropical wave forcing alone is insufficient to explain the signals observed in both the NH polar region during the Boreal winter and spring and the equatorial region during the Austral winter and spring. There must be either extra or different mechanisms at play to cause the incompatible signals in the extratropical NH winter.

5. Summary

By using daily and monthly data extending from 1963 to 2009, we have revealed a significant solar wind dynamics pressure (P_{sw}) relationship to the annual cycle of temperature in the tropical tropopause region, which in turn affects the QBO during Austral late winter and spring. The main characteristics of this relationship can be summarized as follows.

1) A significant change in both the strength and phase occurrence frequency of the QBO in the lower stratosphere are found in the lower stratosphere in relation to the solar wind dynamic pressure. The signature is manifested by stronger and more frequent occurrence of easterly anomalies associated with high P_{sw} during July-October in the lower stratosphere. The effect is related to much higher frequency variations of P_{sw} than the 11-year solar cycle and the most significant response is found at 30-50 hPa.
2) The annual averaged vertical profile of the tropical zonal wind anomalies caused by P_{sw} perturbation is characterized by a vertical three-cell anomaly pattern with westerly anomalies in the troposphere, easterly anomalies at 20-70 hPa and westerly anomalies at 3-10 hPa. Despite its smaller amplitude in comparison to those obtained from Austral winter and spring months, this well-structured wind anomaly pattern is statistically significant all-year around. There is additional seasonal variation superimposed on this annual average with noticeable upward movement during the Boreal winter and spring and downward movement during the Austral late winter and spring, consistent with the known annual cycle effect with stronger upwelling during NH winter and weaker upwelling during SH winter.
3) The tropical temperature response to P_{sw} is characterized by anomalous warming of 2 K at 30-50 hPa and up to 1 K near the tropopause during the Boreal winter and spring

accompanied by up to 0.5 K cooling in the troposphere during the Austral winter and spring. There is an anomalous downward propagation of positive temperature anomalies from the upper stratosphere to the lower stratosphere over a period of a year starting from December. The combined effect may cause a systematic modulation of the annual cycle in the tropical stratospheric temperature and wind.

It remains to be understood what mechanism can cause the observed seasonal modulation of the annual cycle by solar wind dynamic pressure leading to statistically significant changes of the QBO. As the annual cycle in tropical temperature and zonal wind is strongly coupled to the annual cycle in stratospheric water vapour, ozone and wave activity from the troposphere [*Mote et al*., 1995; *Fueglistaler et al*., 2009], a next step would be to look for changes in convective water vapour, ozone and/or upward propagating equatorial waves. Through such related research, the pathways by which the effect of solar wind variability, which is observable mainly in the lower thermosphere and above, may propagate to the lower atmosphere can be better understood.

Acknowledgements

We are very grateful to three anonymous reviewers for their constructive and insightful comments, which helped to reshape the original manuscript. We also thank Peter Kirsch at British Antarctic Survey for help with acquiring and managing the ERA-40 and ECWMF Operational data.

References

Arnold, N. F., and T. R. Robinson (2001), Solar magnetic flux influences on the dynamics of the winter middle atmosphere, *Geophys. Res. Lett.*, *28*(12), 2381-2384.

Baldwin, M. P., and L. J. Gray (2005), Tropical stratospheric zonal winds in ECMWF ERA-40 reanalysis, rocketsonde data, and rawinsonde data, *Geophys. Res. Lett.*, *32*(9), art. no.-L09806.

Baldwin, M. P., et al. (2001), The quasi-biennial oscillation, *Reviews of Geophysics*, *39*(2), 179-229.

Christiansen, B. (2010), Stratospheric bimodality: Can the equatorial QBO explain the regime behavior of the NH winter vortex?, *J. Clim.*, *23*, 3953-3966.

Cordero, E. C., and T. R. Nathan (2005), A new pathway for communicating the 11-year solar cycle signal to the QBO, *Geophys. Res. Lett.*, *32*, L18805, doi:18810.11029/12005GL023696.

Crooks, S. A., and L. J. Gray (2005), Characterization of the 11-year solar signal using a multiple regression analysis of the ERA-40 dataset, *J. Clim.*, *18*(7), 996-1015.

de Artigasa, M. Z., and A. Elias (2005), The equatorial stratospheric QBO and geomagnetic activity, *J. Atmos. Sol.-Terr. Phys.*, *67*, 1280–1286.

Dunkerton, T. J. (1983), Modification of stratospheric circulation by race constituent changes?, *J. Geophys. Res.*, *88*, 10 831–810 836.

Dunkerton, T. J. (1990), Annual variation of deseasonalized mean flow acceleration the the equatorial lower stratosphere, *J. Meteor. Soc. Japan*, *68*, 499-508.

Dunkerton, T. J. (1991), Nonlinear propagation of zonal winds in an atmosphere with Newtonian cooling and equatorial wavedriving, *J. Atmos. Sci.*, *48*, 236–263.

Dunkerton, T. J. (2000), Inferences about QBO dynamics from the atmospheric ‘‘Tape Recorder’’ effect, *J. Atmos. Sci.*, *57*, 230-245.

Dunkerton, T. J., and D. P. Delisi (1997), Interaction of the quasi-biennial oscillation and stratopause semiannual oscillation, *J. Geophys. Res.*, *102*(D22), 26,107–26.

Fischer, P., and K. K. Tung (2008), A reexamination of the QBO period modulation by the solar cycle, *J. Geophys. Res.*, *113*, D07114, doi:07110.01029/02007JD008983.

Fueglistaler, S., A. E. Dessler, T. J. Dunkerton, I. Folkins, Q. Fu, and P. W. Mote (2009), Tropical tropopause layer, *Rev. Geophys.*, *47*, RG1004, doi:1010.1029/2008RG000267.

Gray, L. J., et al. (2010), Solar influence on climate, *Rev. Geophys.*, doi:10.1029/2009RG000282.

Gray, L. J., S. J. Phipps, T. J. Dunkerton, M. P. Baldwin, E. F. Drysdale, and M. R. Allen (2001), A data study of the influence of the equatorial upper stratosphere on northern-hemisphere stratospheric sudden warmings, *Q. J. R. Meteorol. Soc.*, *127*(576), 1985-2003.

Haigh, J. D. (2003), The effects of solar variability on the Earth's climate, *Philos. Trans. R. Soc. Lond. Ser. A-Math. Phys. Eng. Sci.*, *361*(1802), 95-111.

Hamilton, K. (2002), A note on the quasi-decadal modulation of the stratospheric QBO period, *J. Clim.*, *15,* 2562-2565.

Hampson, J., and P. Haynes (2004), Phase alignment of the tropical stratospheric QBO in the annual cycle. *J. Atmos. Sci.*, *61*, 2627–2637.

Holton, J. R., and R. S. Lindzen (1972), An updated theory for the quasi biennial oscillation of the tropical stratosphere, *J. Atmos. Sci.*, *29,* 1076-1080.

Holton, J. R., P. H. Haynes, M. E. Mcintyre, A. R. Douglass, R. B. Rood, and L. Pfister (1995), Stratosphere-troposphere exchange, *Reviews of Geophysics*, *33,* 403-439.

Hood, L. L. (2004), Effects of solar UV variability on the stratosphere, in *Solar variability and its effect on the Earth.s atmosphere and climate system*, edited by J. Pap, P. Fox, C. Frolich, H. Hudson, J. Kuhn, J. McCormack, G. R. North, W. Sprigg and S. Wu, AGU Monograph Series, Washington D.C.

Jarvis, M. J. (1996), Quasi-Biennial Oscillation effects in the semidiurnal tide of the Antarctic lower thermosphere, *Geophys. Res. Lett.*, 23(19), 2661–2664, doi:10.1029/96GL02394.

Kane, R. P. (2005), Differences in the quasi-biennial oscillation and quasi-triennial oscillation characteristics of the solar, interplanetary, and terrestrial parameters, *J. Geophys. Res.*, *110,* A01108, doi:01110.01029/02004JA010606.

King, J. H., and N. E. Papitashvili (2005), Solar wind spatial scales in and comparisons of hourly Wind and ACE plasma and magnetic field data, *J. Geophys. Res.*, *110,* A02104, doi:02110.01029/02004JA010649.

Kinnersley, J. S., and S. Pawson (1996), The descent rates of the shear zones of the equatorial QBO, *J. Atmos. Sci.*, *53*, 1937–1949.

Kodera, K., and Y. Kuroda (2002), Dynamical response to the solar cycle, *J. Geophys. Res.*, *107*(D24), D4749, doi:4710.1029/2002JD002224.

Kuai, L., R.-L. Shia, X. Jiang, K. K. Tung, and Y. L. Yung (2009a), Modulation of the period of the Quasi-Biennial Oscillation by the solar cycle, *J. Atmos. Sci.*, *66*(8), 2418-2428.

Kuai, L., R. L. Shia, X. Jiang, K. K. Tung, and Y. L. Yung (2009b), Nonstationary Synchronization of Equatorial QBO with SAO in Observations and a Model, *J. Atmos. Sci.*, *66*, 1654–1664.

Labitzke, K., M. Kunze, and S. Bronnimann (2006), Sunspots, the QBO and the stratosphere in the North Polar Region - 20 years later, *Meteorol. Zeitschrift*, *15*, 355-363.

Langematz, U., J. L. Grenfell, K. Matthes, P. Mieth, M. Kunze, B. Steil, and C. Brühl (2005), Chemical effects in 11-year solar cycle simulations with the Freie Universität Berlin Climate Middle Atmosphere Model with online chemistry (FUB-CMAM-CHEM), *Geophys. Res. Lett.*, *32*, L13803, doi:13810.11029/12005GL022686.

Lockwood, M., Bell, C., T. Woollings, R. G. Harrison, L. J. Gray, and J. D. Haigh (2010a), Top-down solar modulation of climate: Evidence for centennial-scale change, *Environ. Res. Lett.*, *5*, 034008, doi:034010.031088/031748-039326/034005/034003/034008.

Lockwood, M., R. G. Harrison, T. Woollings, S. K. Solanki (2010b), Are cold winters in Europe associated with low solar activity? *Environ. Res. Lett. 5*, 024001.

Lu , B. W., L. Pandolfo, K. Hamilton (2009), Nonlinear representation of the quasi-biennial oscillation. *J Atmos Sci*., *66*, 1886–1904.

Lu, H., M. J. Jarvis, and R. E. Hibbins (2008a), Possible solar wind effect on the Northern Annular Mode and northern hemispheric circulation during winter and spring, *J. Geophys. Res.*, *113*, D23104, doi:23110.21029/12008JD010848.

Lu, H., M. A. Clilverd, A. Seppälä, and L. L. Hood (2008b), Geomagnetic perturbations on stratospheric circulation in late winter and spring, *J. Geophys. Res.*, *113*, D16106, doi:16110.11029/12007JD008915.

Lu, H., M. J. Jarvis, H. F. Graf, P. C. Young, and R. B. Horne (2007), Atmospheric temperature response to solar irradiance and geomagnetic activity, *J. Geophys. Res.*, *112*, D11109, doi:11110.11029/12006JD007864.

Mayr, H. G., J. G. Mengel, and C. L. Wolff (2005), Wave-driven equatorial annual oscillation induced and modulated by the solar cycle, *Geophys. Res. Lett.*, *32*, L20811, doi:20810.21029/22005GL023090.

Mayr, H. G., J. G. Mengel, C. L. Wolff, and H. S. Porter (2006), QBO as potential amplifier of solar cycle influence, *Geophys. Res. Lett.*, *33*, L05812, doi:05810.01029/02005GL025650.

McCormack, J. P. (2003), The influence of the 11-year solar cycle on the quasi-biennial oscillation, *Geophys. Res. Lett.*, *30*(22), 2162, doi:2110.1029/2003GL018314.

McCormack, J. P., D. E. Siskind, and L. L. Hood (2007), Solar-QBO interaction and its impact on stratospheric ozone in a zonally averaged photochemical transport model of the middle atmosphere, *J. Geophys. Res.*, *112*, D16109, doi:16110.11029/12006JD008369.

Mote, P. W., K. H. Rosenlof, J. R. Holton, R. S. Harwood, and J. W. Waters (1995), Seasonal-Variations of Water-Vapor in the Tropical Lower Stratosphere, *Geophys. Res. Lett.*, *22*(9), 1093-1096.

Nathan, T. R., and E. C. Cordero (2007), An ozone-modified refractive index for vertically propagating planetary waves, *J. Geophys. Res.*, *112*, D02105, doi:02110.01029/02006JD007357.

Naujokat, B. (1986), An update of the observed quasi-biennial oscillation of the stratospheric winds over the tropics., *J. Atmos. Sci.*, *43*, 1873-1877.

Norton, W. A. (2006), Tropical wave driving of the annual cycle in tropical tropopause temperatures. Part II: Model results, *J. Atmos. Sci.*, *63*, 1420–1431.

Palmer, M. A., and L. J. Gray (2005), Modeling the atmospheric response to solar irradiance changes using a GCM with a realistic QBO, *Geophys. Res. Lett.*, *32*(24).

Pascoe, C. L., L. J. Gray, S. A. Crooks, M. N. Juckes, and M. P. Baldwin (2005), The quasi-biennial oscillation: Analysis using ERA-40 data, *J. Geophys. Res.*, *110*(D8), D08105, doi:08110.01029/02004JD004941.

Plumb, R. A., and R. C. Bell (1982), A model of the quasi-biennial oscillation on an equatorial beta-plane, *Q. J. R. Meteorol. Soc.*, *108*, 335-352.

Punge, H. J., and M. A. Giorgetta (2007), Differences between the QBO in the first and in the second half of the ERA-40 reanalysis, *Atmos. Chem. Phys*., 7, 599–608.

Randall, C.E., V.L. Harvey, G.L. Manney, Y. Orsolini, M. Codrescu, C. Sioris, S. Brohede, C.S. Haley, L.L. Gordley, J.M. Zawodny, and J.M. Russell (2005), Stratospheric effects of energetic particle precipitation in 2003-2004, *Geophys. Res. Lett.*, *32* (5), L05802, doi:10.1029/2004GL022003.

Randall, C.E., V.L. Harvey, C.S. Singleton, S.M. Bailey, P.F. Bernath, M. Codrescu, H. Nakajima, and J.M. Russell III (2007), Energetic particle precipitation effects on the Southern Hemisphere stratosphere in 1992–2005, , *J. Geophys. Res.*, *112*, D08308, doi:10.1029/2006JD007696.

Randall, C.E., V.L. Harvey, C.S. Singleton, P.F. Bernath, C.D. Boone, and J.U. Kozyra (2006), Enhanced NO_x in 2006 linked to strong upper stratospheric Arctic vortex, *Geophys. Res. Lett.*, *33*, L18811, doi:10.1029/2006GL027160.

Randel, W. J., R. R. Garcia, N. Calvo, and D. Marsh (2009), ENSO influence on zonal mean temperature and ozone in the tropical lower stratosphere, *Geophys. Res. Lett.*, 36, L15822, doi:10.1029/2009GL039343.

Randel, W. J., F. Wu, J. M. Russel III, A. Roche, J. W. Waters (1998), Seasonal cycles and QBO variations in stratospheric CH_4 and H_2O observed in UARS HALOE data, *J. Atmos. Sci.*, *55*, 163-185.

Randel, W. J., F. Wu, S. J. Oltmans, K. H. Rosenlof, and G. E. Nedoluha (2004), Interannual changes of stratospheric water vapor and correlations with tropical tropopause temperatures, *J. Atmos. Sci.*, *61*, 2133–2148.

Rosenlof, K. H. (1995), Seasonal cycle of the residual mean meridional circulation in the stratosphere, *J. Geophys. Res.*, *100*(D3), 5173–5191, doi:5110.1029/5194JD03122.

Rozanov, E., L. Callis, M. Schlesinger, F. Yang, N. Andronova, and V. Zubov (2005), Atmospheric response to NO_y source due to energetic electron precipitation, *Geophys. Res. Lett.*, *32*(14), L14811, doi:10.1029/2005GL023041.

Salby, M., and P. Callaghan (2000), Connection between the solar cycle and the QBO: The missing link, *J. Clim.*, *13*(14), 2652-2662.

Seppälä, A., C. E. Randall, M. A. Clilverd, E. Rozanov, and C. J. Rodger (2009), Geomagnetic activity and polar surface air temperature variability, *J. Geophys. Res.*, 114, A10312, doi:10.1029/2008JA014029.

Seppälä, A., P.T. Verronen, M.A. Clilverd, C.E. Randall, J. Tamminen, V. Sofieva, L. Backman, and E. Kyrölä (2007), Arctic and Antarctic polar winter NO_X and energetic particle precipitation in 2002-2006, *Geophys. Res. Lett.*, *34*, L12810, doi:10.1029/2007GL029733.

Siskind, D.E., S.D. Eckermann, L. Coy, J.P. McCormack, and C.E. Randall (2007), On recent interannual variability of the Arctic winter mesosphere: Implications for tracer descent, *Geophys. Res. Lett.*, *34*, L09806, doi:10.1029/2007GL029293.

Solomon, S., P.J. Crutzen, and R.G. Roble, Photochemical coupling between the thermosphere and the lower atmosphere: 1. Odd nitrogen from 50 to 120 km, *J. Geophys. Res.*, *87*, 7206-7220, 1982.

Soukharev, B. E., and L. L. Hood (2001), Possible solar modulation of the equatorial quasi-biennial oscillation: Additional statistical evidence, *J. Geophys. Res.*, *106*(D14), 14855-14868.

Sugiura, M., and D. J. Poros (1977), Solar-Generated Quasi-Biennial Geomagnetic Variation, *J. geophys. Res.*, *82*, 5621–5628.

Taguchi, M. (2009), Wave driving in the tropical lower stratosphere as simulated by WACCM. Part I: Annual cycle, *J. Atmos. Sci.*, *66*, 2029–2043.

Uppala, S. M., et al. (2005), The ERA-40 reanalysis, *Q. J. R. Meteorol. Soc.*, *131*(612), 2961-3012.

Wang, M., J. E. Overland, D. B. Percival, and H. O. Mofjeld (2006), Change in the Arctic influence on Bering Sea climate during the twentieth century, *Int J Climatol*, *26*(4), 531-539.

Woollings, T., M. Lockwood, G. Masato, C. Bell, and L. Gray (2010), Enhanced signature of solar variability in Eurasian winter climate, *Geophys. Res. Lett.*, *37*, L20805, doi:20810.21029/22010GL044601.

Yulaeva, E., J. R. Holton, and J. M. Wallace (1994), On the cause of the annual cycle in tropical lower stratospheric temperature, *J. Atmos. Sci.*, *51*, 169-174.

Figure Captions

Figure 1. Height-time cross section of the monthly-mean zonal wind (top two panels) and the QBO time series (*i.e.* de-seasonalized monthly mean zonal mean zonal wind averaged over 5°S-5°N) (bottom two panels) for the period of 1958-2009. Red and blue colors represent westerly and easterly winds respectively.

Figure 2. Time series of monthly solar wind dynamic pressure P_{sw} (blue line), with its high & low frequency components shown as the red and dark solid black lines. The frequency separation is done by treating the original monthly P_{sw} with an order 11 Butterworth high-pass filter with a cut-off period of 36 months.

Figure 3. The QBO phase occurrences under HP (1st row), and under LP (2nd row) at 70-30 hPa pressure levels (from left to right), calculated based on daily data. Westerly winds (wQBO) are donated as solid lines and easterly winds (eQBO) are donated as gray shaded and dashed contour lines. wQBO and eQBO are defined as > 0.25 and < -0.25 of the normalized monthly mean of the QBO.

Figure 4. The QBO phase occurrences in relation to high (HP, solid line with +) and low (LP, dashed line with o) solar wind dynamic pressure for eQBO (1st row), under wQBO (2nd row) phases at 70-30 hPa pressure levels (from left to right). HP and LP are defined as > 0.25 and < -0.25 of the normalized monthly P_{sw} median.

Figure 5. (a) Vertical profile of the annual mean tropical wind (solid line) and ± one standard deviation (dotted lines); (b) Departure from the annual mean for HP and LP conditions (solid lines) for the period of 1963-2009; (c) same as (b) but based on data from 1979-2009; (d) same as (b) but based on data when two years after each major volcanic eruption are excluded. In (b), (c) and (d), 95% confidence intervals are shown as dotted lines for both HP and LP conditions. When the dotted lines do not overlap, it indicates that the average

differences between the HP and LP groups are significant at or above the 95% confidence level. All the departures are calculated as deviations from the monthly mean based on daily data which is then aggregated to give the annual mean departure.

Figure 6. Same as figure 5b but for December-February (a), March-May (b), June-August (c), and September-November (d) means. The departures from the seasonal means are calculated based on daily data aggregated into a seasonal mean departure. The usage of the lines and the definition of significant levels are the same as figure 5.

Figure 7. Height-time cross section of running composite difference of the daily equatorial zonal wind (in m s^{-1}) from 1^{st} of June to 30^{th} of October for HP-LP condition. A 31-day running window is applied to both the wind and P_{sw} without any time lag. (a): the linear regression is based on raw P_{sw}. (b): A high-pass filter with cut-off period of 1095-day (~3-years). (c): same as (b) but data affected by the major volcanic eruptions are excluded. (d): same as (b) but data affected by the major El Niño (1972, 1973, 1982, 1983, 1997, and 1998) are excluded.

Figure 8. Correlations between the July to October averaged high frequency P_{sw} (*i.e.* with period shorter than 3 years, denoted as $P_{sw\ \mathrm{JASO}}$) and the averaged QBO for the same calendar months (denoted as $\mathrm{QBO}_{\mathrm{JASO}}$) at 50 hPa (a) and 30 hPa (b), respectively. Individual years are shown as two digital numbers. Years affected by major volcanic eruptions and major El Niño events are highlighted as red and green squares. The correlation coefficient, statistical confidence level (in brackets), and number of samples used are given in the top of the panels (also in brackets).

Figure 9. Same as Figure 7(a), except that the equatorial zonal-mean zonal wind is replaced by equatorial zonal-mean temperature and the x-axis are extended from 1^{st} of the January to 31^{st} of the December and y-axis from 1000 hPa to 1 hPa.

Figure 10. (a) Vertical profile of tropical (5°S-5°N) climatological mean annual pattern of zonal-mean zonal wind in m s^{-1}. Westerly winds are donated as solid lines and easterly winds are donated as gray shaded and dashed contour lines. (b) Vertical profile of tropical climatological mean annual variation of temperature (thick black lines, lower panel) and temperature anomalies from annual mean profile (shaded contour) in K. Negative temperature anomalies are donated with gray shading.

Figure 11. Histograms of the QBO phase transitions (zero crossings based on daily data) at 10hPa, 20hPa, 30hPa, 50hPa and 70hPa (top to bottom) grouped by month. Westerly to easterly transitions are displayed in the left-hand panels, while easterly to westerly transitions are shown in the right-hand panels. The climatology and variability faster than 6 months were removed before the transitions were determined. The years of the transitions are donated by two digital numbers.

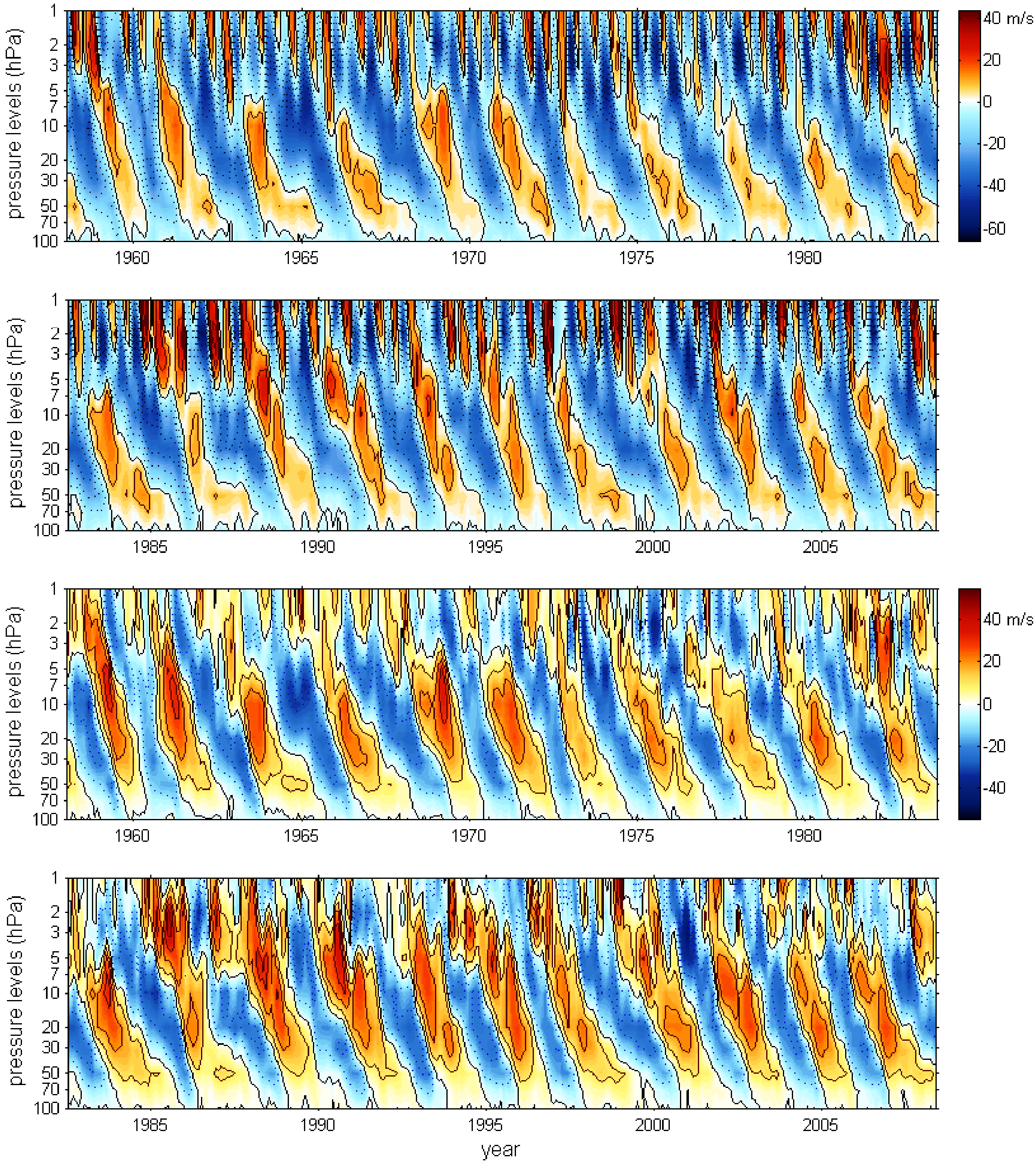

pressure levels (hPa)
1
2
3
5
7
10
20
30
50
70
100
1960
1965
1970
1975
1980
1985
1990
1995
2000
2005
40 m/s
20
0
-20
-40
-60
year

Figure 1

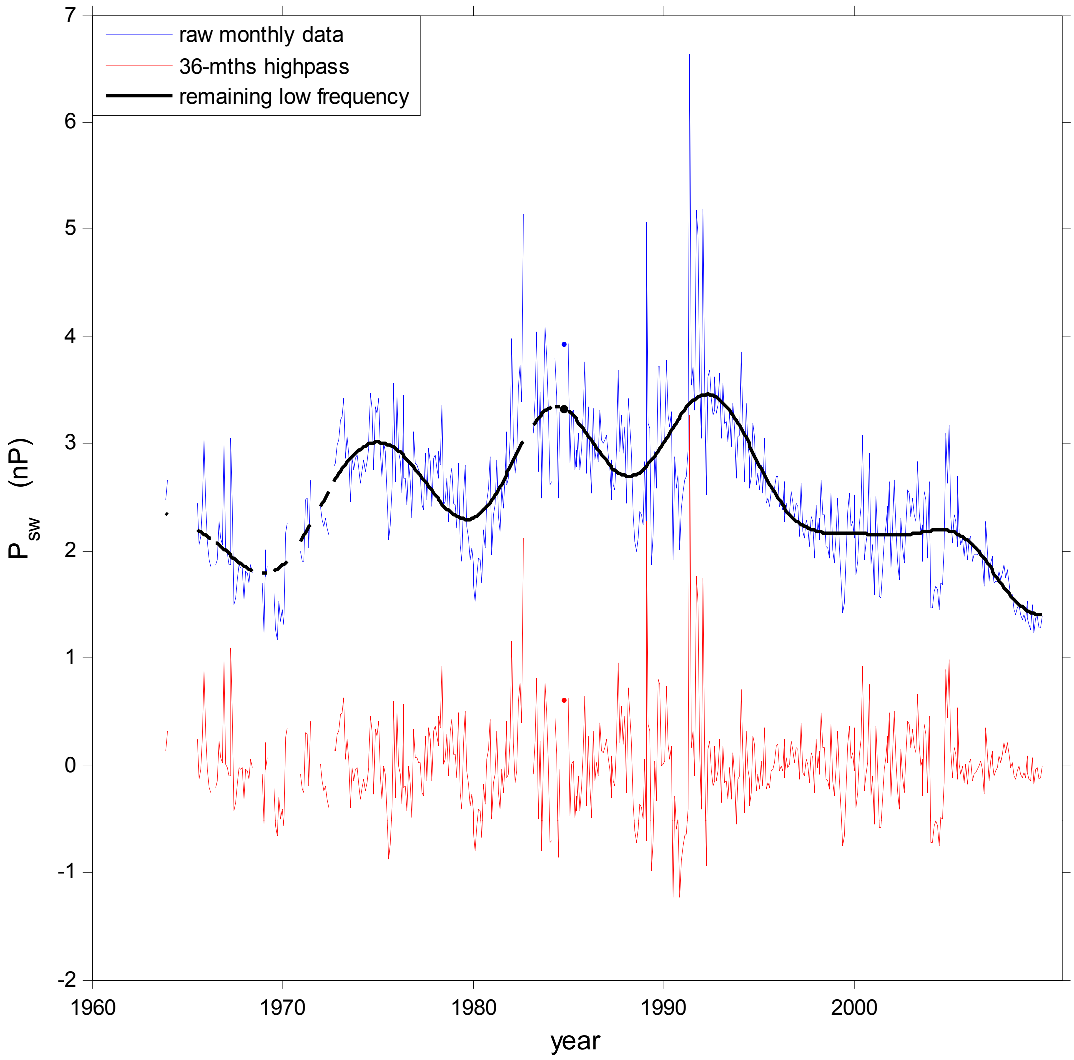
raw monthly data
36-mths highpass
remaining low frequency
7
6
5
4
3
2
1
0
-1
-2
P_{sw} (nP)
1960
1970
1980
1990
2000
year

Figure 2

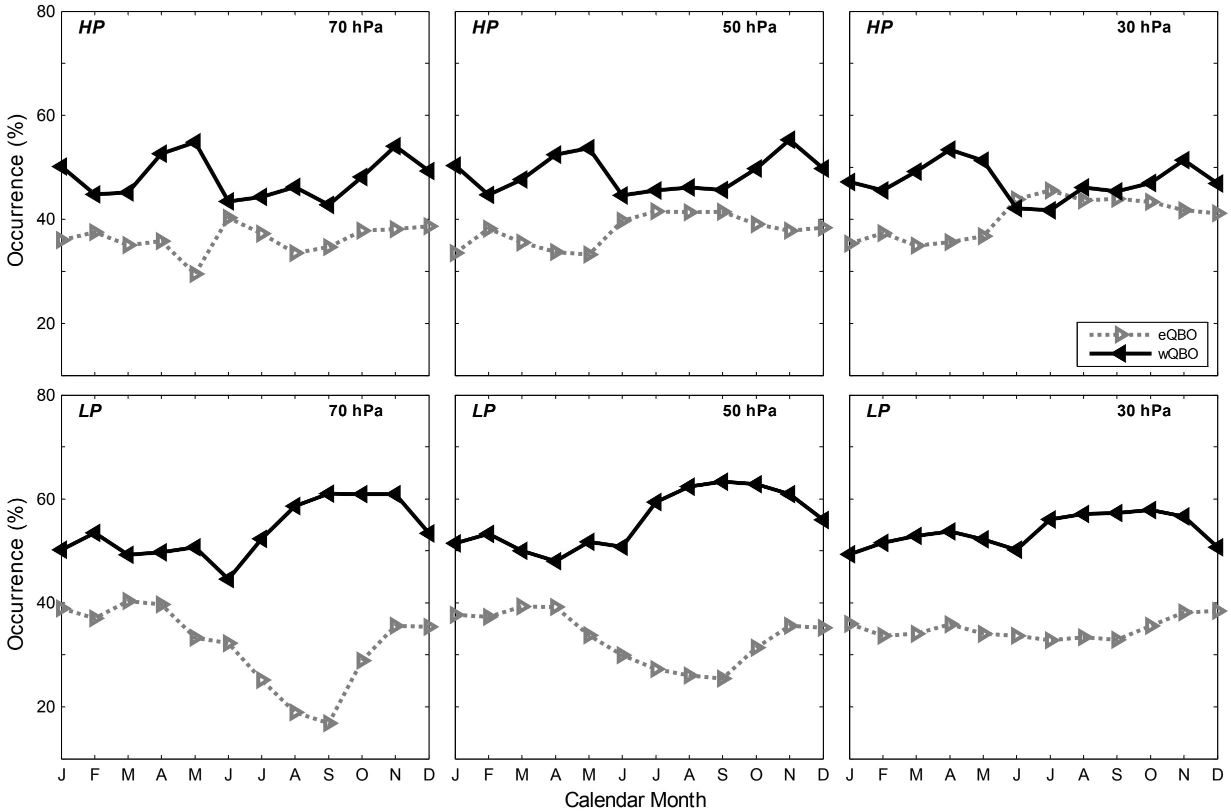
HP
70 hPa
HP
50 hPa
HP
30 hPa
LP
70 hPa
LP
50 hPa
LP
30 hPa
eQBO
wQBO
Occurrence (%)
Calendar Month
J F M A M J J A S O N D

Figure 3

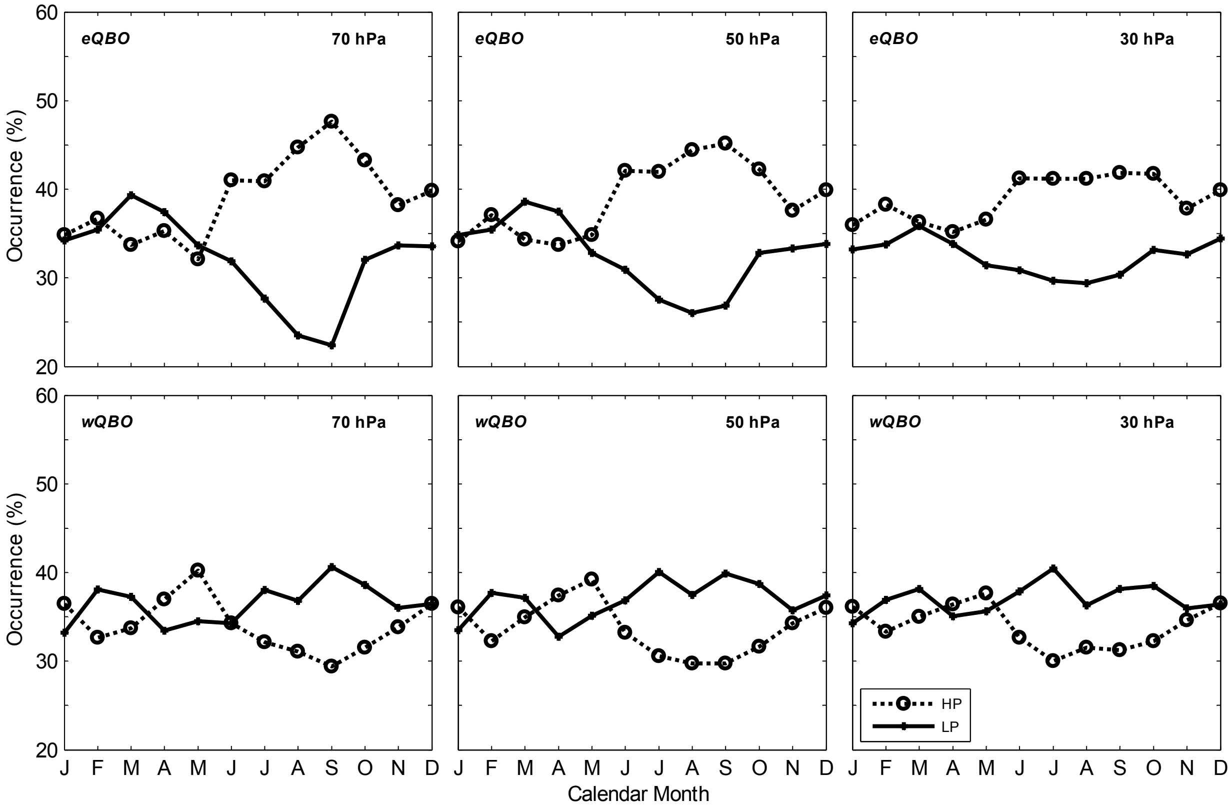

60
50
40
30
20
Occurrence (%)
eQBO
70 hPa
50 hPa
30 hPa
wQBO
HP
LP
J F M A M J J A S O N D
Calendar Month

Figure 4

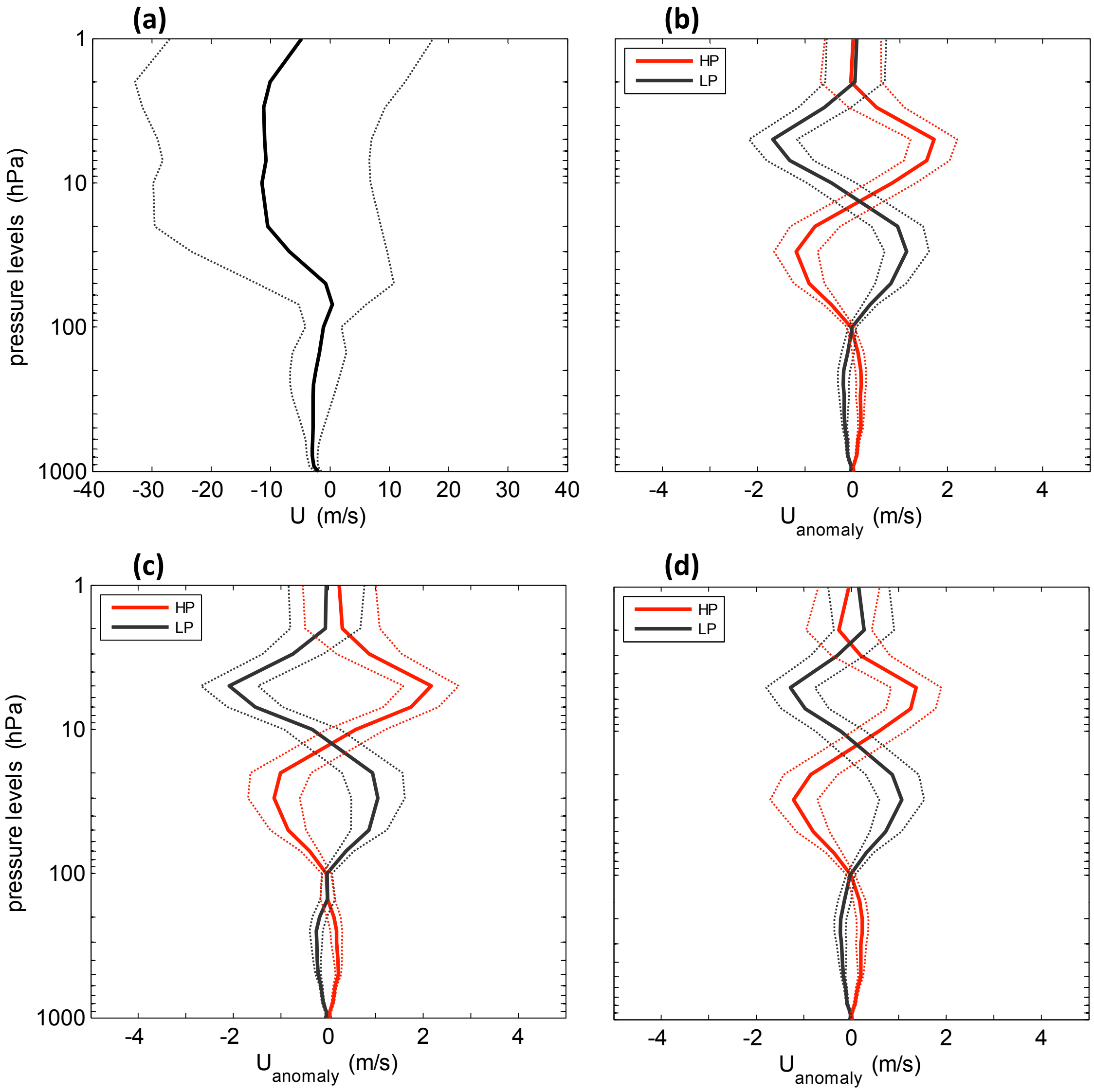
(a)
(b)
(c)
(d)
pressure levels (hPa)
1
10
100
1000
-40
-30
-20
-10
0
10
20
30
40
U (m/s)
HP
LP
-4
-2
0
2
4
U anomaly (m/s)

Figure 5

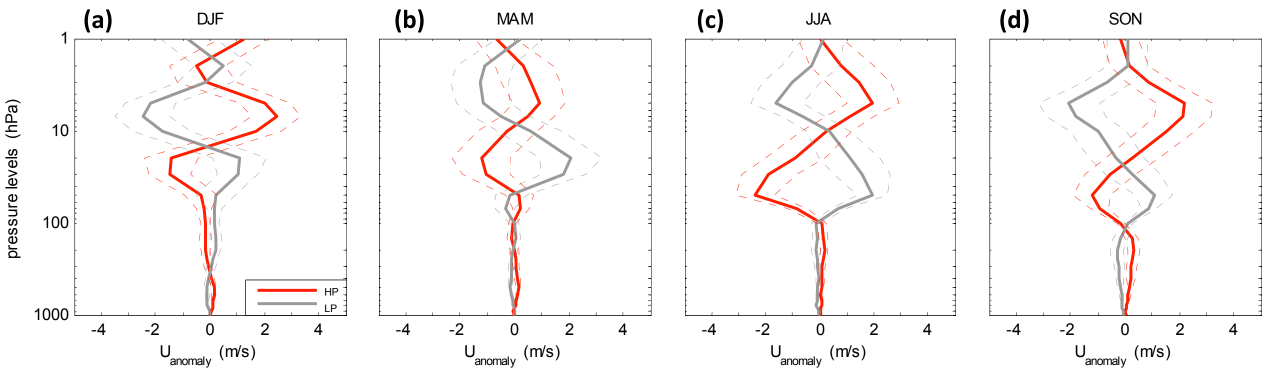
(a)
DJF
(b)
MAM
(c)
JJA
(d)
SON
pressure levels (hPa)
1
10
100
1000
HP
LP
-4
-2
0
2
4
$U_{anomaly}$ (m/s)

Figure 6

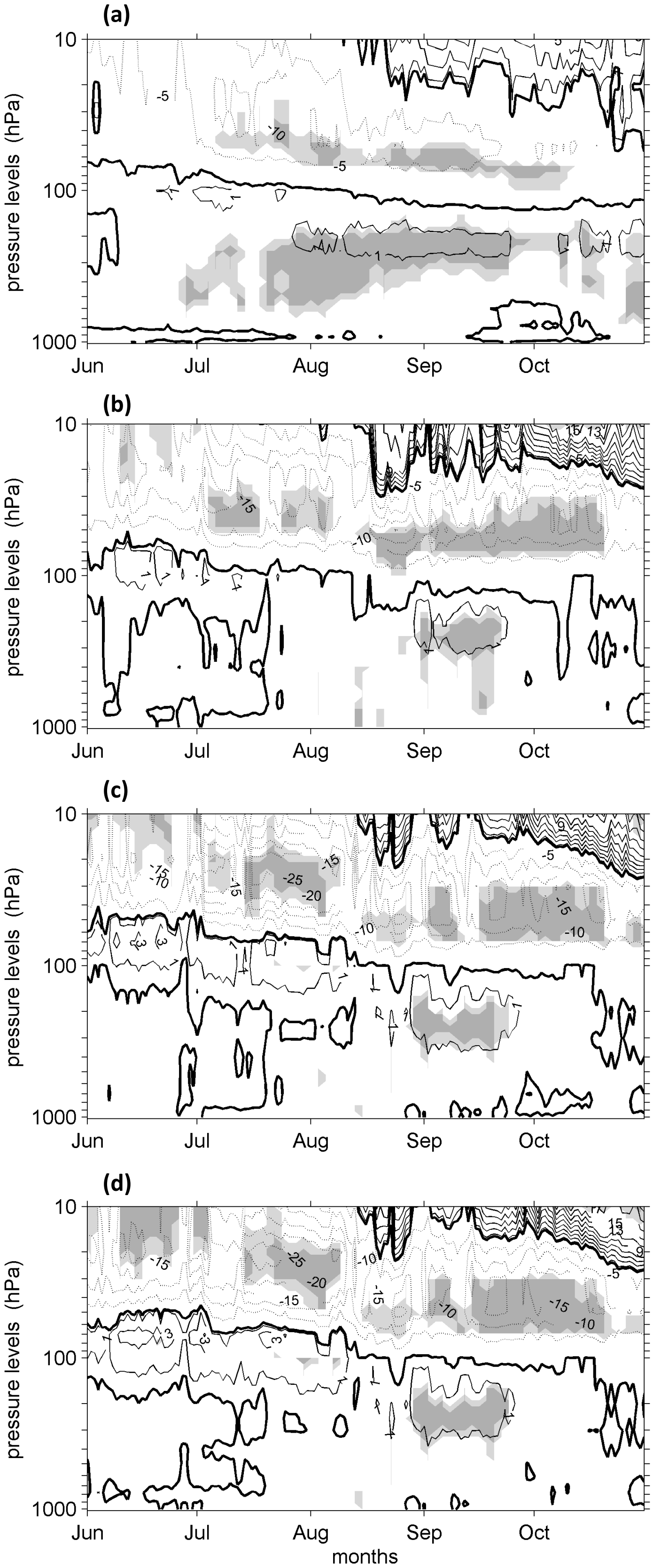

(a)
(b)
(c)
(d)
pressure levels (hPa)
10
100
1000
Jun
Jul
Aug
Sep
Oct
months

Figure 7

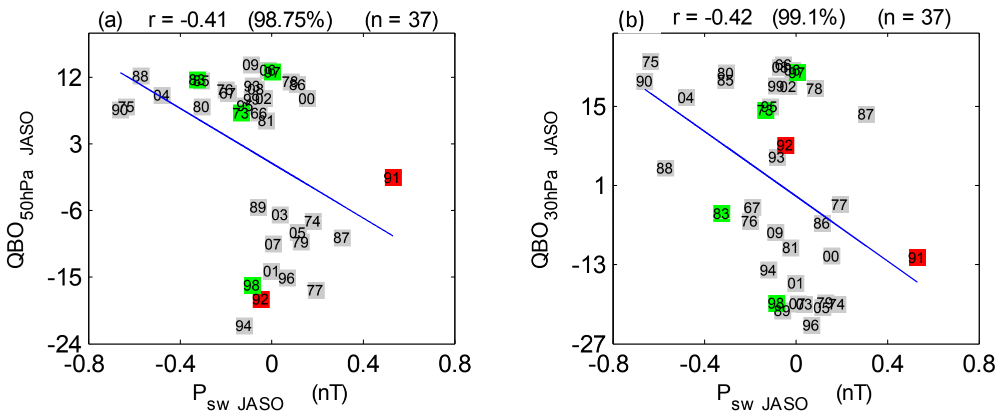
(a) r = -0.41 (98.75%) (n = 37)
QBO50hPa JASO
Psw JASO (nT)
(b) r = -0.42 (99.1%) (n = 37)
QBO30hPa JASO
Psw JASO (nT)

Figure 8

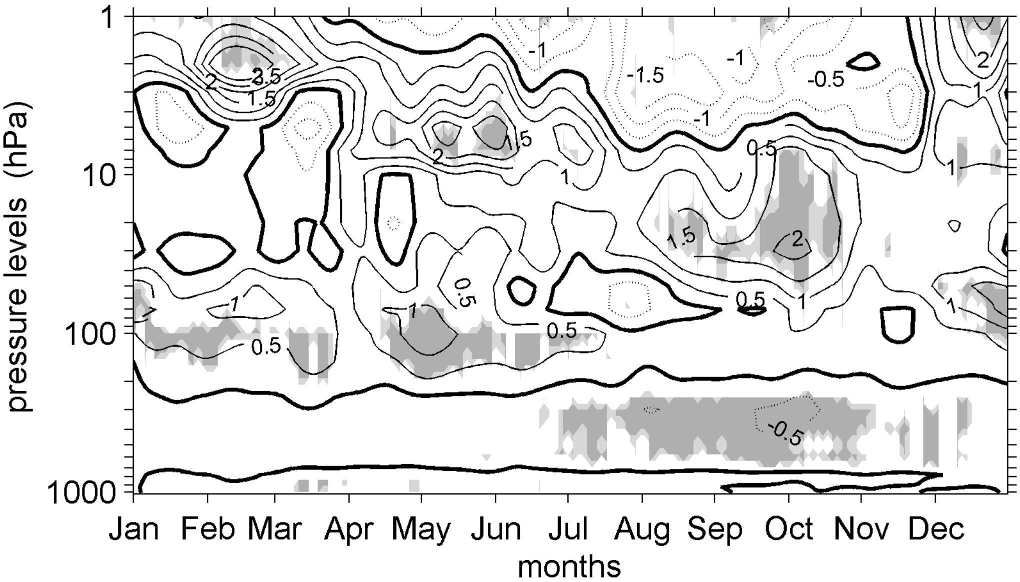

pressure levels (hPa)
1
10
100
1000
Jan
Feb
Mar
Apr
May
Jun
Jul
Aug
Sep
Oct
Nov
Dec
months

Figure 9

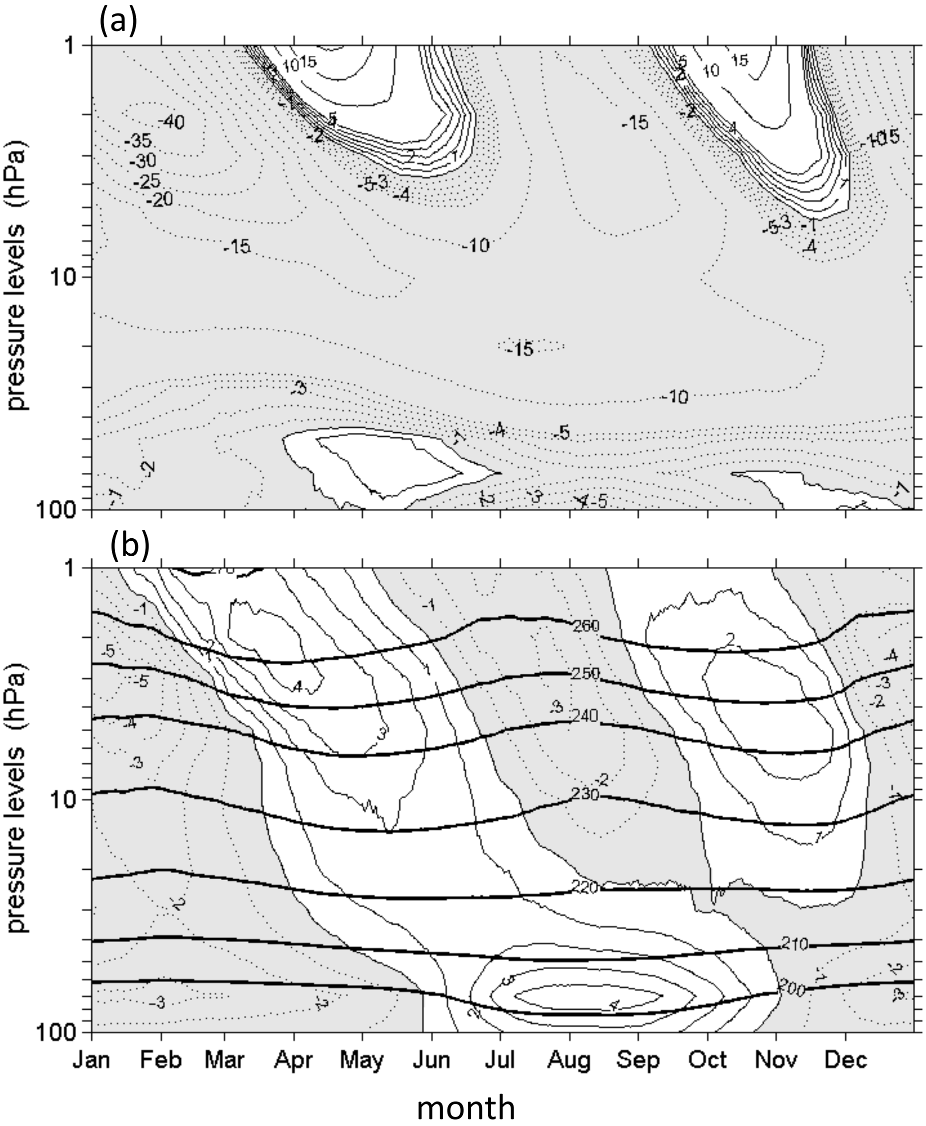
(a)
(b)
pressure levels (hPa)
1
10
100
Jan
Feb
Mar
Apr
May
Jun
Jul
Aug
Sep
Oct
Nov
Dec
month

Figure 10

Westerly->Easterly

10 hPa

J	F	M	A	M	J	J	A	S	O	N	D
									06		
									04		
									90		
									80		
								85	75		
					02			69	61		
		88		95	99		08	66	59		
64		83	93	78	73		97	57	55		

20 hPa

J	F	M	A	M	J	J	A	S	O	N	D
										06	
				83						04	97
		09		67						02	85
		86	91	64	93				95	99	61
58	60	72	88	53	76			78	73	69	55

30 hPa

J	F	M	A	M	J	J	A	S	O	N	D
		07		00							
	74	05		91	09						88
03	65	79	62	81	86	83					69
98	56	60	58	72	67	76			93	95	53

50 hPa

J	F	M	A	M	J	J	A	S	O	N	D
					07						
					03						
			98	05	91						
			96	70	89						
			94	65	79						
		01	84	60	74	62					
77	87	68	54	56	72	58					81

70 hPa

J	F	M	A	M	J	J	A	S	O	N	D
					98			05			
					96			79			
					84	01		74			
		92			78	73		71	07	08	
		82	87		70	72		65	89	03	
63		77	68	94	60	56		54	58	91	

Easterly->Westerly

10 hPa

J	F	M	A	M	J	J	A	S	O	N	D
				03							
				98						00	
				94						81	
				84	07			05		76	
				68	96	70	79	91	72	62	
		87		54	89	56	74	60	65	58	

20 hPa

J	F	M	A	M	J	J	A	S	O	N	D
										07	
										05	
								03		89	
							96	98		79	
86	75			92	87	01	68	84	96	72	
66	59			63	82	77	54	60	70	56	

30 hPa

J	F	M	A	M	J	J	A	S	O	N	D
04											
97											
80	08					92					
73	90					87					
71	69		75			82				01	98
57	61	06	66	59		63		77	94	54	84

50 hPa

J	F	M	A	M	J	J	A	S	O	N	D
				08	90						
				06	80						
		02	04	97	69						
		99	85	71	66	75			87		
95	78	55	73	61	57	59		63	82		92

70 hPa

J	F	M	A	M	J	J	A	S	O	N	D
						07			75		
				99	06	85			66		
	93			95	97	78	90		59	87	91
09	55	53		73	69	71	80	61	57	63	82

Figure 11